Subproject A2.6

Optimized Quantum Dots for Spin Devices and Optimized Resonators

Principle Investigator: Daniel M. Schaadt

CFN-Financed Scientists: M. Helfrich (1/2 E13, 36 months)

Further Scientists: D. Litvinov, E. Müller, D. Z. Hu

DFG-Centrum für Funktionelle Nanostrukturen (CFN)
Karlsruher Institut für Technologie (KIT)

Optimized Quantum Dots for Spin Devices and Optimized Resonators

Introduction and Summary

Semiconductor quantum dots (QDs) consist of islands of a small bandgap semiconductor which are embedded in a matrix of a larger bandgap semiconductor. Due to its confinement potential with discrete energy levels this system is termed an artificial atom. These nanometer sized islands exhibit various interesting physical phenomenae: they can produce single photons [1], entangled photon pairs [2] or store spins [3].

Access to single dots is required, and thus a low dot density, in order to assess these physical properties. This can be achieved by either placing metal masks on the sample to select the emission of only a few dots, or better, by adjusting growth conditions to obtain a low density directly. Using molecular beam epitaxy we previously found a new annealing regime, where the dot size and shape remain constant while the composition decreases with annealing time [4,5]. The quantum dots fabricated in this manner show a relatively low In concentration of around 30%, which is beneficial for spintronics applications. Injected spins are thereby less affected through the nuclear spins in the In ions [6]. We are growing quantum dots using this annealing regime and optimize their properties for use in spin devices.

To allow for a manipulation and control of the spin state or coupling to a resonator, well defined quantum dots are required which can be placed at the correct location between leads in spin devices or at locations of high field intensities in resonator structures. The self-assembled nucleation of quantum dots is inherently a random process. Preferential nucleation can be achieved, however, by creating small dips on the surface [7]. This method alone still leads to a fairly large dot distribution with dots nucleating not all at desired locations but also in-between or by forming clusters of multiple dots instead of a single dot [8]. However, in combination with annealing procedures that were investigated previously, we anticipate a much higher control over dot nucleation, thereby removing interstitials or multiple dots. Our technique is illustrated in Fig. 1.

Electron beam lithography is used to define small dips in a GaAs substrate. Wet-chemical etching is currently used to transfer the dips from the resist into the substrate. Once the equipment is available we will switch to dry etching for better control of very small dip sizes. InAs quantum dots are then grown by molecular beam epitaxy on the pre-structured substrates. This is followed by *in-situ* annealing.

Using well designed patterns in combination with annealing will further allow us to prepare large, asymmetrically shaped dots with higher oscillator strength for better coupling to resonator structures used in subproject A2.3 (H. Kalt, M. Hetterich).

In the timeframe 2008-2010 we have established a reproducible process for sample pre-structuring which was continuously optimized. Additionally, site-selective quantum dots were grown on pre-structured substrates and characterized by means of atomic force microscopy (AFM; in collaboration with Prof. Schimmel), photoluminescence spectroscopy (μ-PL; in collaboration with Prof. Kalt and Prof. Gibbs and Prof. Khitrova, University of Arizona) and transmission electron microscopy (TEM; in collaboration with Prof. Gerthsen). Furthermore, we have started to investigate the effect of *in-situ* annealing on site-selective quantum dots. First results are described hereafter.

Subproject A2.6 has led to 3 publications in 2010.

Fig. 1: Concept for optimized quantum dots. The substrate is pre-structure by electron beam lithography (a). This is followed by removal of the surface oxide and growth of a thin buffer layer (b). Quantum dots preferentially nucleate in the dips, but interstitials can be present as well as multiple dots per site (c). Annealing is used to control the quantum dot distribution and properties (d).

1. Substrate Pre-Structuring by Electron Beam Lithography

Techniques to precisely position QDs have been elaborated in the past. Top-down techniques such as electron beam lithography (EBL), local oxidation or mechanical nano-indentation have proven to be viable in order to define QD nucleation sites [9,10,11]. Common to those approaches is the creation of small holes on the substrate surface, which leads to selective QD nucleation at the desired locations. Pre-structuring is commonly performed *ex-situ* and usually involves several process steps. Besides intended surface manipulation, contamination can occur. Therefore, great care has to be taken with regard to surface cleanliness prior to regrowth in order to inhibit unintended QD nucleation caused by defects.

Epi-ready (100) GaAs wafers are used as substrates and surface pre-structuring is performed on top of a GaAs epitaxial layer. Conventional electron-beam lithography is used to define 50-70 nm wide holes in a PMMA/MA (polymethyl methacrylate/methacrylate) co-polymer resist on the surface. The holes are arranged on square grids with varying lattice constants. They are etched about 30 nm deep into the substrate by wet chemical etching using H_2SO_4:H_2O_2:H_2O. The resist is then removed and the samples are cleaned in a series of solvent baths. Figure 2 depicts a pre-structured area of a GaAs substrate.

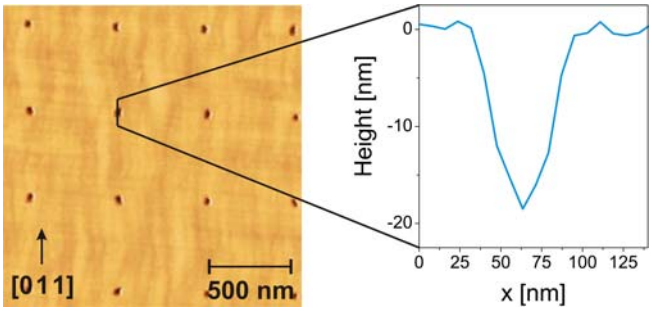

Fig. 2: AFM image of pre-structured GaAs surface with a representative linescan through a dip. The depth is less than 30 nm which might be due to the AFM tip size or lower etch rate than calibrated [12].

In the beginning, additional unintended holes were found on the substrate surface after regrowing a thin GaAs buffer layer on top of the pre-structured samples [12,13]. These "defect" holes were related to incomplete surface cleaning and interfere with the attempt of deterministic QD nucleation, since they act as nucleation sites as well. Such a "defect" hole is shown in the micrograph of Fig. 3, with the GaAs not overgrowing the original GaAs surface in the center.

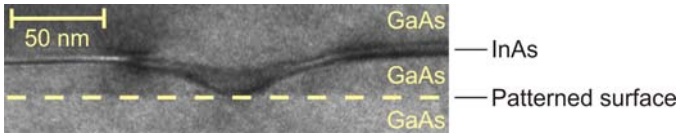

Fig. 3: TEM micrograph of "defect" hole appearing after GaAs regrowth [13].

The sample cleaning procedure was optimized as a consequence and UV/ozone cleaning was introduced in order to remove remaining organic contamination.

Cleaning samples after EBL comprises several steps. First, the resist needs to be removed which is done with an adequate remover. Thereafter, the samples are cleaned with different solvents (trichlorethylene, acetone, isopropyl alcohol, methanol), if possible in a heated ultrasonic bath. Finally, the samples are rinsed in bi-distilled water. The resist used for EBL contains organic compounds. Especially the high temperature during dry-baking of the resist results in a high stability of such compounds against solvents. Critical steps of the cleaning procedure are depicted in Fig. 4.

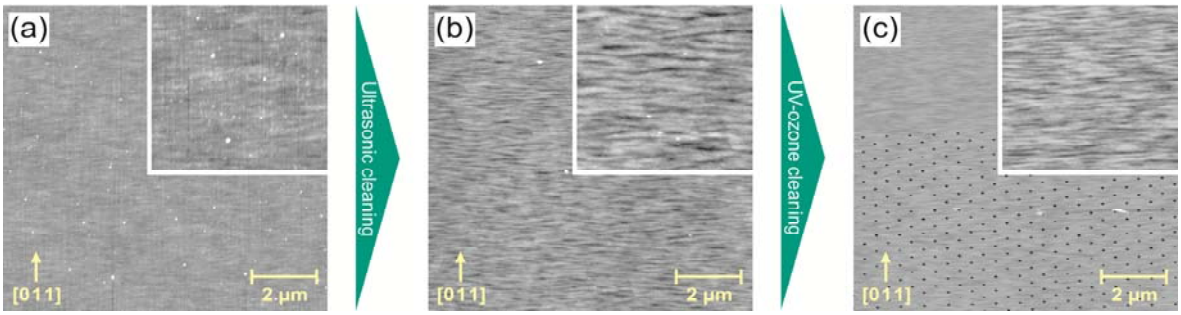

Fig. 4: AFM images of samples at different stages of the cleaning procedure: after cleaning with solvents (a), using a heated ultrasonic bath (b), and after UV/ozone cleaning (c) [13].

The sample in Fig. 4 (a) was cleaned using steps one and two of the above procedure but without ultrasonic bath. A lot of contamination is observed from the AFM image (large particles appearing white). When the samples are cleaned in a heated ultrasonic bath, the amount of contamination is reduced. Especially the amount of smaller particles has decreased, as seen in Fig. 4 (b). However, there are still larger areas of residues remaining on the surface. In order to get rid of these remaining contaminants a UV/ozone cleaning step was introduced. It utilizes a low-pressure mercury lamp that emits radiation at the relevant wavelengths of 184.9 nm and 253.7 nm [14]. Molecular oxygen is dissociated by the shorter wavelength with the atomic oxygen subsequently forming ozone. Ozone is then decomposed by the longer wavelength. Atomic oxygen is thus constantly provided. In addition, the 253.7 nm radiation excites organic molecules. These react with the atomic oxygen and form simpler, volatile compounds that desorb from the surface. The effect of UV/ozone cleaning is displayed in Fig. 4 (c) where essentially all contamination has disappeared. Clean oxygen was fed

throughout the cleaning process. UV/ozone cleaning is a very gentle process which does not bombard the surface with ions. The cleaning efficiency is comparable to conventional plasma ashing.

As a result of the improved sample preparation and cleaning process, the number of defect holes is drastically reduced resulting in a uniform and flat GaAs buffer layer after regrowth, as illustrated in Fig. 5.

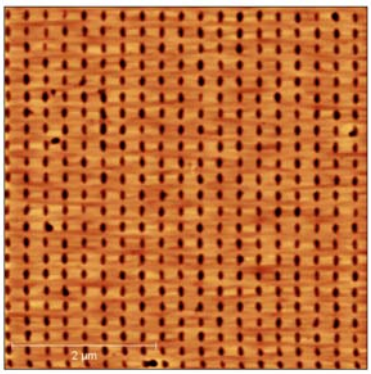

Fig. 5: AFM image of sample after GaAs buffer layer regrowth. The sample was prepared according to the optimized cleaning procedure. InAs was also deposited but no QDs are observed since the critical thickness was not reached.

2. Site-Selective Growth of InAs Quantum Dots via Molecular Beam Epitaxy

Site-selective nucleation of QDs is driven by the local change in the surface chemical potential which is provided through the small dips on the substrate surface. The deformation of the surface alters the chemical potential in such a way that the growth rate is locally increased. Therefore, quantum dots preferentially nucleate inside the dips, as seen in Fig. 6. The predominant double dot formation is probably attributed to a change in the hole shape during GaAs buffer layer overgrowth [15].

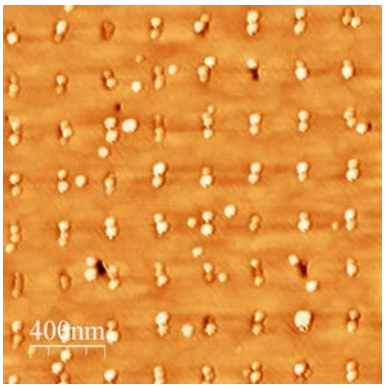

Fig. 6: SEM image of site-selective QDs. The spacing is 250 nm and the nominal InAs thickness is 1.7 ML.

The regular QD pattern is also observed in the TEM image of Fig. 7. The sample is not capped and the QD shape is revealed as pyramidal. It has to be noted that TEM analysis of site-selective QDs has not been reported yet. We will continue investigating the structure of our site-selective QDs by this technique in order to learn more about possible defects in the QDs.

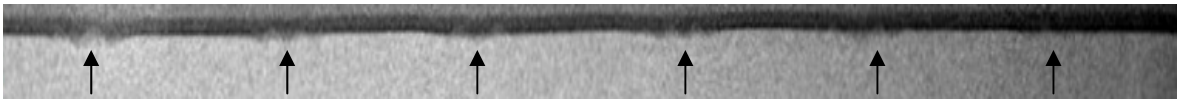

Fig. 7: TEM image of site-selective QDs. Arrows indicate the positions of the QDs. The spacing is 250 nm. The nominal InAs thickness is 1.7 ML. Single and double dot nucleation is observed.

3. *In-situ* Annealing of Site-Selective InAs Quantum Dots via Molecular Beam Epitaxy

Site-selective QDs were annealed and compared to as grown site-selective ones. Figure 8 shows a set of QD samples with both containing 1.7 ML of InAs. The as grown sample shows predominant double dot nucleation per site. QDs nucleating on interstitial sites are found since the supplied amount of InAs is above the critical thickness for QD formation on pre-structured substrates. After annealing the sample for 2:30 min, the number of interstitial QDs is reduced and, moreover, a morphological change of the site-selective QDs is observed [13]. Original double dots merge into single dots. By facilitating In-adatom migration the annealing step causes the material to redistribute. The volume of the newly formed single dots is larger than the combined volume of the original double dots. This is related to the reduction of interstitial dots. The site-selective QDs appear to be more stable than the interstitial dots and ripen by collecting material from surrounding interstitial dots. This observation is best described by a kinetic model with the ripening process being limited by attachment and detachment of atoms on the dot surface [16].

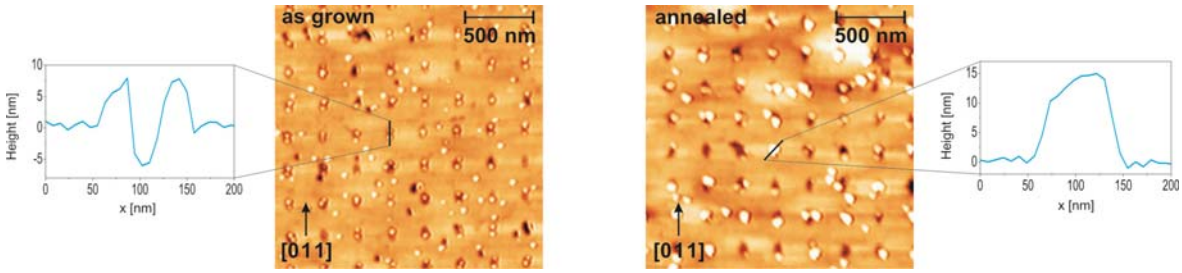

Fig. 8: AFM images of as grown and annealed site-selective QDs. A morphological transition from mainly double dots to single dots is observed after 2:30 min of annealing. Representative linescans support this observation. The nominal InAs thickness is 1.7 ML.

The optical quality of as grown and annealed site-selective QDs was investigated by µ-PL spectroscopy. Representative spectra of an as grown sample capped with 90 nm GaAs is shown in Fig. 9. Luminescence emerging from interstitials could not be discriminated from the one coming from site-selective dots. However, by combining these data with AFM data we were able to perform a statistical analysis and deduce a lower limit of 30% of site-selective QDs being optically active [17].

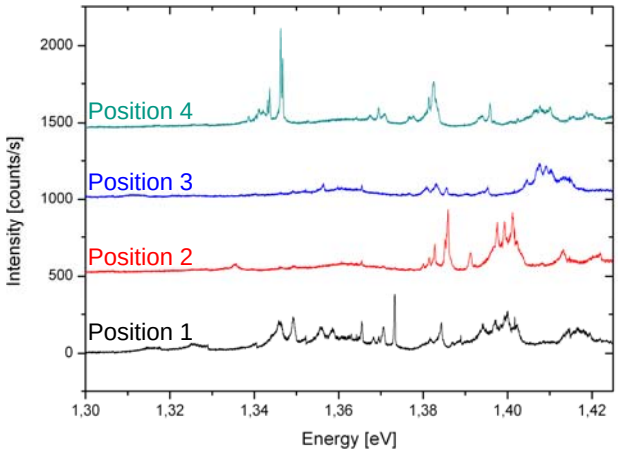

Fig. 9: Micro-PL spectra taken at four different locations within an array with 250 nm spacing [17].

The samples of Fig. 8 were all prepared according to a standard procedure before the optimization of the sample preparation process. That is why many defect holes are present on these samples. After optimization, the number of defects has drastically decreased and QD nucleation is only observed at predefined locations in an array with 250 nm spacing, as seen in Fig. 9. The InAs thickness amounts to 2.6 ML and the sample was annealed for 7:30 min. The absence of interstitials is rather astonishing when bearing in mind the large amount of InAs that was provided here. In addition to the same morphological transition as described above, these results clearly demonstrate the potential of our approach to control QD locations and further properties in site-selective growth.

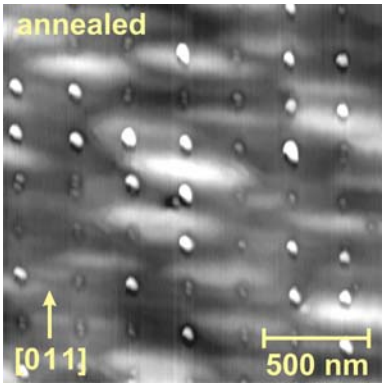

Fig. 10: AFM image of annealed site-selective QDs. 2.6 ML of InAs were deposited and annealed for 7:30 min. Large single dots are observed. Defect holes and interstitials are not present [13].

We will continue investigating the effects of *in-situ* annealing on site-selective quantum dots and possibly insert site-selective QDs in resonator structures.

References

[1] P. Michler, A. Kiraz, C. Becher, W. V. Schoenfeld, P. M. Petroff, L. Zhang, E. Hu and A. Imamoğlu, *Science* **290**, 2282 (2000).

[2] N. Akopian, N. H. Lindner, E. Poem, Y. Berlatzky, J. Avron, D. Gershoni, B. D. Gérardot and P. M. Petroff, *Phys. Rev. Lett.* **96**, 130501 (2006).
[3] M. Kroutvar, Y. Ducommun, D. Heiss, M. Bichler, D. Schuh, G. Abstreiter, and J. J. Finley, *Nature* **432**, 81 (2004).
[4] D. Z. Hu, D. M. Schaadt, and K. H. Ploog, "Stress development during annealing of self-assembled InAs/GaAs quantum dots measured in-situ with a cantilever beam setup," *J. Crystal Growth* **293**, 546 (2006).
[5] D. M. Schaadt, D. Z. Hu, and K. H. Ploog, "Stress evolution during ripening of self-assembled InAs/GaAs quantum dots," *J. Vac. Sci. Technol. B* **24(4)**, 2069 (2006).
[6] M. Yu. Petrov, I. V. Ignatiev, S. V. Poltavtsev, A. Greilich, A. Bauschulte, D. R. Yakovlev, and M. Bayer, *Phys. Rev. B* **78**, 045315 (2008).
[7] S. Jeppesen, M. S. Miller, D. Hessman, B. Kowalski, I. Maximov, and L. Samuelson, *Appl. Phys. Lett.* **68**, 2228 (1996).
[8] P. Atkinson, S. P. Bremner, D. Anderson, G. A. C. Jones, and D. A. Ritchie, *J. Vac. Sci. Technol. B* **24**(3), 1523 (2006).
[9] T. Ishikawa, S. Kohmoto, and K. Asakawa, *App. Phys. Lett.* **73**, 1712 (1998).
[10] J. Martin-Sanchez, Y. Gonzalez, L. Gonzalez, M. Tello, R. Garcia, D. Granados, J. M. Garcia and F. Briones, *J. Cryst. Growth* **284**, 313 (2005).
[11] C. K. Hyon, S. C. Choi, S. H. Song, S. W. Hwang, M. H. Son, D. Ahn, Y. J. Park, and E. K. Kim, *Appl. Phys. Lett.* **77,** 2607 (2000).
[12] M. Helfrich, R. Gröger, A. Förste, D. Litvinov, D. Gerthsen, T. Schimmel, and D. M. Schaadt, "Investigation of pre-structured GaAs surfaces for subsequent site-selective InAs quantum dot growth", *accepted for Nanoscale Res. Lett.* (2010).
[13] M. Helfrich, D. Z. Hu, J. Hendrickson, M. Gehl, D. Rülke, R. Gröger, D. Litvinov, S. Linden, M. Wegener, D. Gerthsen, T. Schimmel, M. Hetterich, H. Kalt, G. Khitrova, H. M. Gibbs, and D. M. Schaadt, "Growth and annealing of InAs quantum dots on pre-structured GaAs substrates", *accepted for J. Crystal Growth* (2010).
[14] S. I. Ingrey, Surface Processing of III-V Semiconductors, in: P. H. Holloway and G. E. McGuire (eds.), *Handbook of Compound Semiconductors*, Noyes Publications, Park Ridge (NJ), 251 (1995).
[15] S. Kiravittaya, H. Heidemeyer, and O. G. Schmidt in: O. G. Schmidt (ed.), *Lateral Alignment of Epitaxial Quantum Dots*, Springer, Berlin, 489 (2007).
[16] D. Z. Hu, D. M. Schaadt and K. H. Ploog, "Stress development during annealing of self-assembled InAs/GaAs quantum dots measured in situ with a cantilever beam setup", *J. Cryst. Growth* **293,** 546 (2006).
[17] J. Hendrickson, M. Helfrich, M. Gehl, D. Z. Hu, D. M. Schaadt, S. Linden, M. Wegener, B. Richardson, H. Gibbs, and G. Khitrova, "InAs quantum dot site-selective growth on GaAs substrates", *accepted for phys. stat. sol.* (2010).